

Numerical Analysis of the Influence of Head Diameter on the Breakout Capacity of Shallow Headed Studs

Jindřich Fornůšek¹, Petr Konvalinka² & John J. Cairns³

Abstract: The aim of this paper is comparison of 2D numerical analysis results of cast-in-place headed studs with different head size and effective embedment depth to the CCD (Concrete Capacity Design) approach that is used for design of anchoring in Eurocode 2. Breakout simulation tests of six different head diameters with four different effective embedment depths were investigated. The concrete properties were kept constant for all of them. It was found that the capacity of anchor is affected by the head size significantly. The approximately 25% decrease of capacity for small heads and about 30% capacity increase for large heads were observed in comparison to the CCD method.

Keywords: Anchorage, Breakout, Capacity, Concrete, Headed Studs, Numerical Simulation, Tension.

1. Introduction

The anchorage systems for concrete structures are well known and tested especially to the bridge engineering where headed studs transfer the shear load from steel girders to concrete slabs. Demands of designers for new fast and flexible technologies of concrete reinforcing and casting moved the anchorage systems to another application like tension and combination of tension and shear in common concrete structures. Therefore deeper investigation of behaviour of these anchorage systems needs to be performed.

Anchor systems for concrete structures can be divided into the two basic classifications: cast-in-place headed studs which are placed to the mould before casting of concrete and post-installed anchors (undercut, expansion and adhesive anchors) which are installed to the drilled hole into hardened concrete [7]. Four types of tensile failure can be identified for these anchorage systems: steel yielding, pulling-out, concrete splitting and concrete breakout [5]. This paper is focused on behaviour of shallow cast-in-place headed studs and those concrete breakout capacity in dependence on the size of the head and the effective depth of anchor especially. The other ways of failure or different types of anchors were not the objective of this paper.

¹ Ing. Jindřich Fornůšek, Experimental Centre, Faculty of Civil Engineering, Czech Technical University in Prague, Thákurova 7, 16629, Prague, Czech Republic, jindrich.fornusek@fsv.cvut.cz

² prof. Petr Konvalinka, Experimental Centre, Faculty of Civil Engineering, Czech Technical University in Prague, Thákurova 7, 16629, Prague, Czech Republic, petr.konvalinka@fsv.cvut.cz

³ dr. John. J. Cairns, School of the Built Environment, Heriot Watt University, EH14 4AS, Edinburgh, Scotland (UK), j.j.cairns@hw.ac.uk

For the prediction of the single anchor breakout capacity can be used the Concrete Capacity Design (CCD) approach as it was shown in [7]. This method is suitable especially for shallow anchors up to 250 mm of effective depth [3]. The numerical simulations of behaviour of large embedded anchors (effective depth varied from 150 mm to 1500 mm) with three different head size types were presented in [9]. These simulations proved that there is about 25% increase of capacity of medium sized head (31 mm) and about 35% increase of capacity of large sized head (40 mm) in comparison to small head (22 mm) for effective depth of 150 mm. The significant increase of capacity in dependence of head size was found also for the others effective depths but for this paper the shallowest effective depth is the most interesting. Unfortunately the influence of the head size on breakout capacity of anchor is not involved in the CCD approach. Hence the more tests and simulations of this influence are necessary to be investigated.

2. Breakout capacity design

As was mentioned above in the introduction the breakout capacity of single anchor can be calculated according to the CCD method. The CCD method is adopted by the ACI 318 [1] and Eurocode 2 [2] hence the emphasis in this paper is given to this method. The CCD breakout capacity of single anchor is based on the presumption that the concrete fails in the shape of pyramid (Fig. 1) with the pyramid base equaled to three times of effective embedment depth ($3h_{ef}$). This presumption corresponds to widespread experimental observations [7]. The equation (1) is based on this presumption and can be used for calculation of breakout capacity of single anchor N_{n0} [7]:

$$N_{n0} = k_{nc} \cdot \sqrt{f_{cc}'} \cdot h_{ef}^{1.5}; \quad (1)$$

with:

- k_{nc} is 15.5 for mean value of cast-in-place anchors,
- f_{cc}' concrete cubic strength [MPa],
- h_{ef} effective depth of anchor [mm].

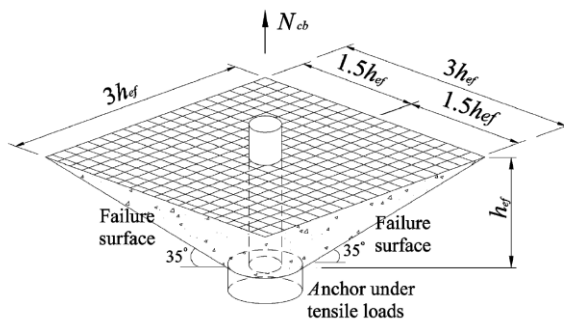


Fig. 1. Idealisation of concrete breakout failure in accordance to the CCD approach [1].

3. Material parameters of numerical model

The commercial software ATENA (Advanced Tool for Engineering Nonlinear Analysis) was used for the solution. The GiD software was used as the pre- and post-processor. Material models for nonlinear behaviour of concrete and steel were part of the used version of the ATENA software.

3.1. Steel material model

The bilinear von Mises plasticity model was used for the modeling of the steel head and the support ring. The yield strength f_y was 550.0 MPa, elasticity modulus E was 210 GPa and hardening modulus H was 10 GPa.

3.2. Concrete material model

The fracture-plastic model Cementitious2 which is included in the ATENA software was selected for the numerical simulation of concrete. This model combines constitutive models for tensile (fracturing) and compressive (plastic) behaviour. It employs Rankine failure criterion, exponential softening and it can be used as rotated or fixed cracks. The hardening/softening plasticity model is based on Menétrey-William failure surface. This model can be used to simulate concrete cracking, crushing under high confinement and crack closure due to crushing in other material directions [6]. The cubic compressive strength was set 30,0 MPa and it was kept constant during all the simulations. The basic parameters of the concrete model are stated below in the Tab. 1.

Table 1. Material parameters of concrete Cementitious2 model

Parameter	Units	Value
Elasticity modulus E	[GPa]	30.32
Poisson coefficient ν	[-]	0.2
Compressive strength f_c	[MPa]	25.5
Tensile strength f_t	[MPa]	2.317

4. Numerical analysis

The 2D axi-symmetric model was carried out because the problem is typically the axi-symmetric task [9]. The variables of simulations were effective depth h_{ef} of anchor, diameter of head d_h and diameter of shank d_d . The head diameter was set in dependence on h_{ef} . The dimensions of h_{ef} , d_h , d_d are specified in Tab. 2.

Table 2. Anchor geometry in dependence on effective depth

h_{ef} [mm]	d_d [mm]	d_h/h_{ef}					
		0.2	0.25	0.3	0.35	0.4	0.45
90	13.5	18	22.5	27	31.5	36	40.5
120	18	24	30	36	42	48	54
150	22.5	30	37.5	45	52.5	60	67.5
200	30	40	50	60	70	80	90
d_h/d_d		1.33	1.67	2	2.33	2.67	3
A_h/A_d		1.77	2.79	4	5.43	7.13	9

4.1. Geometry of the model

The axi-symmetric model consisted of two materials steel - anchor head, support ring and concrete block. The anchor head thickness was 10 mm for all simulations. The support ring's dimensions were set to 50 x 50 mm for almost all of the simulations except $h_{ef} = 200$ mm. In this case the support ring was 100 x 100 mm.

The concrete block's size varied in dependence on effective depth. The scheme of the geometry is shown in the Fig. 2 and the dimensions are stated in the Tab. 3. Concrete block (light grey) was divided into three parts because of different mesh density and dimension c was set to be larger than $1.5h_{ef}$ to ensure the creation of concrete cone (cracks of concrete) in fine density mesh.

Table 3. Dimensions of numerical model

h_{ef} [mm]	a [mm]	b [mm]	c [mm]	h_{ef}/c [-]
90	425	500	250	2.8
120	425	500	300	2.5
150	500	500	350	2.4
200	600	600	450	2.25

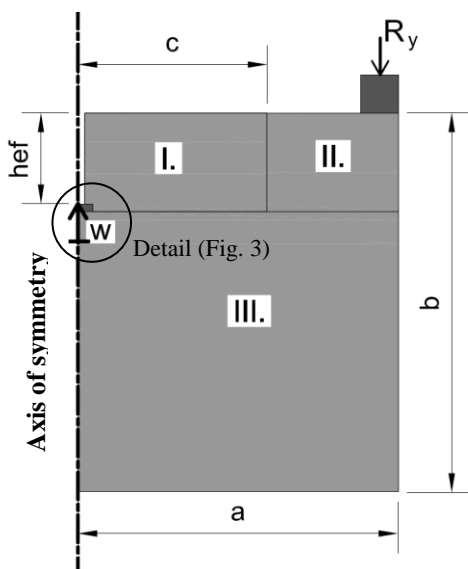


Fig. 2. The scheme of numerical model geometry (light grey–concrete, dark grey– steel)

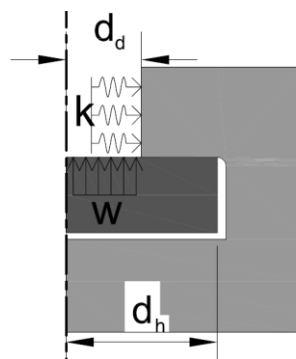


Fig. 3. Detail of the anchor head (light grey– concrete, dark grey– steel head)

4.2. Boundary conditions of the model

The model was supported by the reaction R_y which was set on the support ring and by the axis of symmetry. The displacement w was gradually applied (in 40 – 80 steps) on the shank area of the head (Fig. 3) to simulate the progressive loading. The maximum displacement varied from 1.0 mm to 8.0 mm in dependence of effective depth and

head diameter (the smaller displacements were set for the large head diameters). The reaction R_y was monitored during the loading.

Small gap (1 mm) was created between the concrete block and the head on the side and on the bottom of the head to avoid the friction and tension transfer from head to concrete. The head was rigidly connected to the concrete block only on the top.

The spring constraint was created to simulate presence of the shank and to prevent from pushing of concrete into the shank cavity. Multi-linear stiffness k of the spring was selected. The break points of stiffness curve are presented in the Tab 4. Point 1 in the Tab. 4 represents the stiffness of concrete in tension and point 3 and 4 represent behaviour of steel in compression to simulate presence of the shank.

Table 4. Multi-linear parameters of spring

Point	Stress [MPa]	Strain [-]
1	-2.17	-0.000058
2	0	0
3	550	0.00275
4	578	0.025

4.3. Finite element discretization

The unstructured mesh was selected for discretization of the model in all simulations. The mesh was generated by automatic generator which is implemented in pre-processor. Fine mesh with size of elements about 5 mm or less was selected in the area I. (see Fig. 2) where the cracks of concrete were predicted. In the closest vicinity to the head the smaller (approx. 1 mm) elements were generated. The rough mesh – element size between 25-50 mm – was created in the areas II. and III. to save the calculation time.

4.4. Results of numerical analysis

The maximal achieved reactions against head size (ratio d_h/h_{ef}) in comparison to CCD method are stated in Tab. 5. It can be observed that the capacity of the anchor increases significantly with increasing diameter of the head in all cases. The increase is more significant for the anchors with larger effective depth. There can also be seen the significant decrease (between 40 and 20 %) of the anchor capacity in comparison to the CCD method for small headed anchors.

Table 5. Maximal reactions of numerical simulations

		d_h/h_{ef}					
		0.2	0.25	0.3	0.35	0.4	0.45
h_{ef}	CCD	$R_{y,max}$					
[mm]	[kN]	[kN]					
90	72.5	47.4	56.8	69.5	72.1	75.1	80.3
120	111.6	79.7	101.3	110.4	126.3	125.7	132.2
150	156.0	111.6	154.6	174.4	181.2	184.3	202.1
200	240.1	186.5	250.8	277.8	304.4	324.6	345.7

The typical diagram of reaction against displacement is shown in Fig. 4. All head sizes with effective depth $h_{ef} = 120$ mm are presented in this diagram. The stiffer response of the anchor can be observed with the increasing head diameter. This phenomenon was mentioned in [9] and it was noticed for all other effective depths. The maximal reactions are pointed out in the diagram.

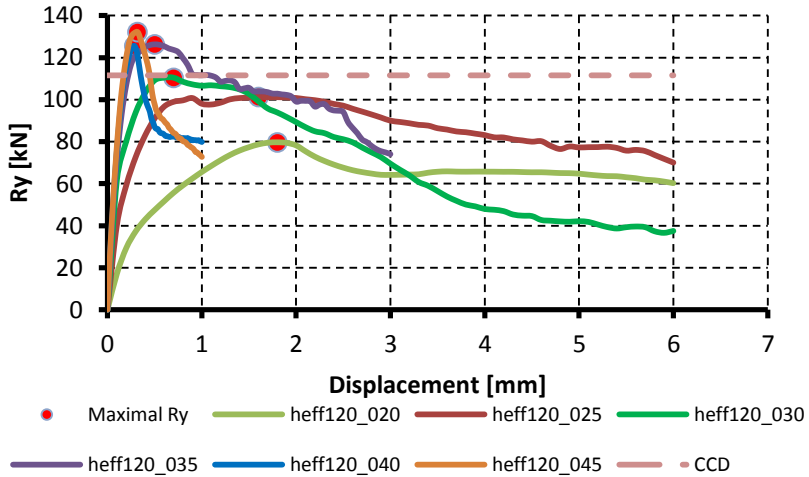


Fig. 4. Typical diagrams of reaction against displacement in dependence on head size.

The two basic modes of concrete cone failure were observed (Fig. 5 and 6). Cracking mode (a) was observed mainly on the shallowest anchors and on the anchors with small head. On the other hand the cracking mode (b) was observed mainly on the anchors with larger effective depth and with large heads. The cracking in the mode (b) progressed in two phases: at first the bottom crack I. was established and then after maximum reaction was achieved the crack II. formed and it was opening till the end of the simulation. The crack I. did not continue in progress after the crack II. had opened. Typical crack pattern can be seen in Fig. 5 ($h_{ef} = 90$ mm; $d_h/h_{ef} = 0.2$) and in Fig. 6 ($h_{ef} = 200$; $d_h/h_{ef} = 0.45$).

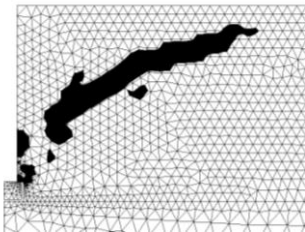


Fig. 5. Typical (a) mode crack - $h_{ef} = 90$ mm; $d_h/h_{ef} = 0.2$.

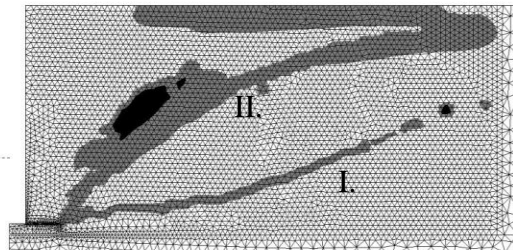


Fig. 6. Typical (b) mode crack - $h_{ef} = 200$; $d_h/h_{ef} = 0.45$.

The bi-linear coefficient k_h which takes into account the influence of the head size was based on the numerical data. This coefficient results from the outcomes of simulation of the model where $h_{ef} = 120$ and $d_h/h_{ef} = 0.3$ (hef120_030). The results of this simulation were almost the same to the CCD approach.

$$k_h = \left(\frac{h_{ef}}{120}\right)^{0.3} \cdot \left(\frac{d_h/h_{ef}}{0.3}\right) \quad \text{for } d_h/h_{ef} < 0.3 \quad (2)$$

$$k_h = \left(\frac{h_{ef}}{120}\right)^{0.3} \cdot \left(\frac{d_h/h_{ef}}{0.3}\right)^{0.5} \quad \text{for } 0.45 \geq d_h/h_{ef} \geq 0.3 \quad (3)$$

The use of equation (3) is limited to $d_h/h_{ef} = 0.45$ because up to this values the simulations have not been executed. The same value should be used for the ratio larger than 0.45 (Fig. 7).

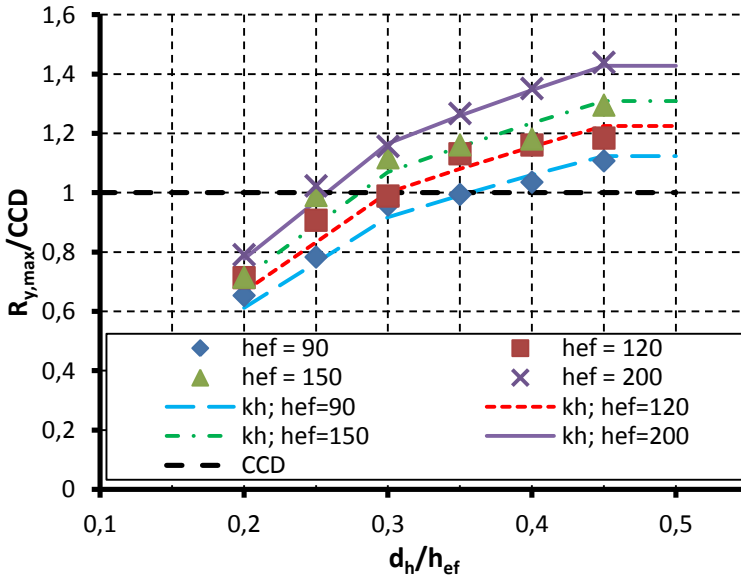


Fig. 7. Maximal reactions R_y and coefficient of head size influence k_h

5. Conclusions

Twenty-four numerical simulations of headed studs with different effective depth and head diameter were investigated in this research. The findings can be summarized in the next four points:

- The simulations approved that size of the head has significant influence on the capacity of anchor in tension. It was found that for the small heads of

anchor can be the CCD approach unsafe and for the large heads is this approach quite conservative.

- The stiffer response with the increasing head size of the anchor can be observed. This phenomenon was observed in all simulations.
- The two different basic modes of concrete cracking were observed in dependence of head size and effective depth.
- The coefficient of head size influence k_h was created based on the numerical data. This coefficient increases/decreases the capacity of anchor according to the CCD.

It has to be stated that these findings are based only on theoretical numerical research. The more theoretical and mainly experimental research should be made to improve the validity of these findings and to refine the CCD approach.

Acknowledgements

This research has been supported by project of the Czech Scientific Foundation No: GD103/09/H078 and by the project of Ministry of Education of the Czech Republic No: MSM6840770031.

References

- [1] ACI Committee 318, "Appendix D – Anchoring to Concrete", *Building Code Requirements for Structural Concrete and Commentary*, ISBN-10: 9780870312649.
- [2] BS EN 1992-1-1:2004, (2004), "Eurocode 2: Design of concrete structures — Part 1-1: General rules and rules for buildings", British Standards Institute, London.
- [3] Cannon R., (1995), "Discussion to the paper Concrete Capacity Design (CCD) Approach for Fastening to Concrete", *ACI Structural Journal*, November - December, pp. 787-791.
- [4] Cannon R., (1996), "Straight Talk about Anchorage to Concrete – Part I", *ACI Structural Journal*, 92-S56, pp. 580-586.
- [5] CEB-fib, (1997), "Design of Fastening in Concrete: Design Guide", Thomas Telford, London, UK.
- [6] Červenka V., Jendele L. and Červenka J., (2009), "ATENA Program Documentation Part 1 – Theory", Červenka Consulting Ltd., Prague.
- [7] Fuchs W., Eligehausen R. and Breen J.E., (1995), "Concrete Capacity Design (CCD) Approach for Fastening to Concrete", *ACI Structural Journal*, 92-S9, pp. 73-94.
- [8] Ožbolt J., Eligehausen R., Periškić G and Mayer U., (2007), "3D FE analysis of anchor bolts with large embedment depth", *Engineering Fracture Mechanics*, 74, pp. 168-178.
- [9] Pivonka P., Lackner R and Mang H.A., (2004), "Concrete Subjected to Tri-axial Stress States: Application to Pull-Out Analysis", *Journal of Engineering Mechanics*, December, pp. 1486-1498.